Hydrodynamic Transport Parameters for Holes in Strained Silicon

F. M. Bufler[1] and B. Meinerzhagen[2]

[1]Institut für Integrierte Systeme
ETH Zürich, Gloriastrasse 35, CH-8092 Zürich, Switzerland
Phone: +41-1-632-5401, Fax: +41-1-632-1194,
E-mail: bufler@iis.ee.ethz.ch

[2]Institut für Theoretische Elektrotechnik und Mikroelektronik
Universität Bremen, D-28334 Bremen, Germany

Drift velocities, carrier temperatures and energy relaxation times are computed by full-band Monte Carlo simulation along the $\langle 110 \rangle$ field direction at 300 K for holes in unstrained and (001)-strained Si grown on a $Si_{0.7}Ge_{0.3}$ substrate. The drift velocity as a function of the electric field is significantly enhanced under biaxial tensile strain, but is smaller than in the unstrained case when plotted versus the hole temperature because the holes are more easily heated under strain. The ohmic in-plane drift mobility and the transient velocity overshoot peak for a sudden application of a field of 100 kV/cm are enhanced by a factor of approximately three and two, respectively.

1. Introduction

Strained Si is one of the most promising materials for strongly enhanced performance of p–MOSFET devices among the various SiGe heterostructures under investigation for this purpose. Improved transport properties of p–MOSFETs under biaxial tensile strain, caused by growing a thin Si layer on a relaxed SiGe buffer or using stress–enhancing isolation processes in pure Si structures, have already been demonstrated experimentally [1, 2]. Theoretical work on hole transport in strained Si has been restricted to low fields [3, 4, 5], apart from Ref. [6], where the velocity–field characteristics along the $\langle 100 \rangle$ and $\langle 001 \rangle$ directions in (001)-strained Si were reported. However, enhanced hole transport in submicron p–MOSFETs based on strained Si will be characterized by ballistic overshoot effects, and hence classical device simulation must also include the energy balance equations. It is therefore the aim of this paper to provide hydrodynamic hole transport parameters for strained Si, e.g. the velocity–temperature relation and the energy relaxation time, by full–band Monte Carlo simulation and to discuss the underlying physics of the partly surprising results.

2. Model and Verification

The material investigated is (001)-strained Si grown on an unstrained $Si_{0.7}Ge_{0.3}$ substrate, being the configuration desired from growth and performance considerations. Biaxial tensile strain is due to the lattice mismatch between the relaxed SiGe buffer, which determines the in–plane lattice constant of the strained layer, and the unstrained Si layer, the relation of which is $a_{SiGe}/a_{Si} = 1.011$ in the above situation. The band structure is obtained from nonlocal empirical pseudopotential calculations [7], where, in addition to Ref. [7], the spin–orbit interaction in Si is also taken into account. The mesh spacing in wave vector space is 0.0125 $(2\pi/a)$, yielding negligible discretization errors. It can be seen in the energy dispersion in Fig. 1 that the main effect of the strain is to lift the degeneracy at the Γ–point, with the light hole band being situated at the valence band edge. The other important aspect for a realistic transport model for holes in strained Si consists of an accurate phonon system. Here, acoustic phonons in the elastic equipartition approximation and optical phonons are considered, assuming the influence of strain to be negligible. The non-vanishing diagonal components of the ohmic drift mobility tensor can be calculated under nondegenerate conditions for this phonon model according to [8, 9]

$$\mu_{i,i} = \frac{q \sum_n \int_0^\infty \tau_{tot}(\epsilon) \mathcal{V}_{i,n}^2(\epsilon) \mathcal{D}_n(\epsilon) e^{-\epsilon/(k_B T_0)} d\epsilon}{k_B T_0 \sum_n \int_0^\infty \mathcal{D}_n(\epsilon) e^{-\epsilon/(k_B T_0)} d\epsilon} \qquad (1)$$

where q is the elementary charge, k_B the Boltzmann constant and T_0 the lattice temperature. $\tau_{tot}(\epsilon)$ denotes the microscopic relaxation time which is given by the inverse total scattering rate. The definitions of the density of states per spin and the ith component of the square of

0-7803-4369-7/98 $10.00

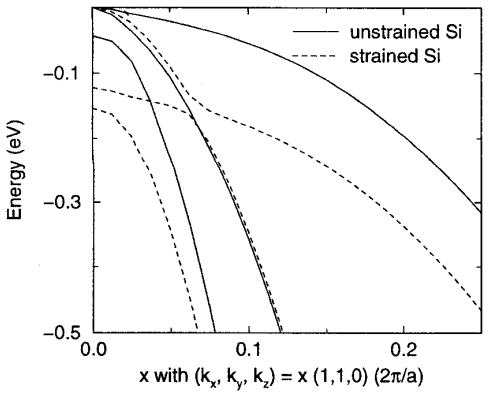

Figure 1: Valence–band energies along the ⟨110⟩ wave–vector direction in unstrained Si and in (001)-strained Si grown on unstrained $Si_{0.7}Ge_{0.3}$

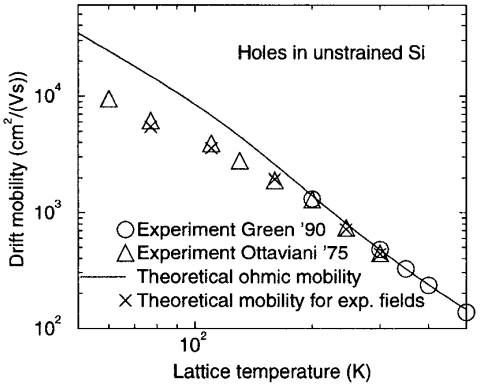

Figure 2: Comparison of the theoretical drift mobility in unstrained Si at different lattice temperatures with corresponding experimental data [10, 11]

the group velocity averaged over an equienergetic surface are for each band n

$$\mathcal{D}_n(\epsilon) \equiv \frac{1}{(2\pi)^3} \int_{\mathrm{BZ}} \delta(\epsilon - \epsilon_n(\mathbf{k})) d^3k \qquad (2)$$

and

$$\mathcal{V}^2_{i,n}(\epsilon) \equiv \frac{\int_{\mathrm{BZ}} v^2_{i,n}(\mathbf{k}) \delta(\epsilon - \epsilon_n(\mathbf{k})) d^3k}{\int_{\mathrm{BZ}} \delta(\epsilon - \epsilon_n(\mathbf{k})) d^3k}, \qquad (3)$$

respectively. Thus, the full bandstructure can be incorporated in the ohmic mobility calculation without any approximations in a very computationally efficient manner. The details of the full-band Monte Carlo simulations in the nonlinear regime are reported elsewhere [9]. The phonon system significantly influences both the lattice temperature dependence and the strain dependence of the mobility. For a verification of the transport model, the theoretical drift mobility at low fields is therefore compared in unstrained Si as a function of the lattice temperature with corresponding experimental results [10, 11]

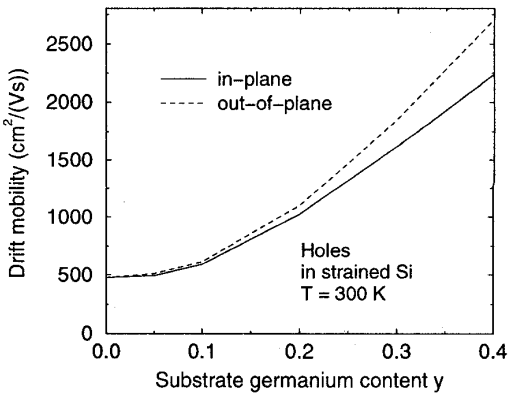

Figure 3: Ohmic in–plane and out–of–plane drift mobility at 300 K for holes in a strained Si layer grown on an (001) $Si_{1-y}Ge_y$ substrate

in Fig. 2. Concerning the time–of–flight measurements [11], it was found that the fields applied in these experiments were too high for the ohmic regime below 200 K. When performing full–band Monte Carlo simulations for those cases at exactly the same fields, a very good agreement between theory and experiment is achieved over the whole range of lattice temperatures. In addition, the Monte Carlo model specified above has been shown to reproduce the experimental velocity–field characteristics in unstrained Si at different lattice temperatures to a high degree of accuracy [9].

3. Results

The effect of the strain-induced band-splitting, which leaves only the light hole band at the valence band edge and reduces intervalley scattering, clearly shows up in the ohmic drift mobility displayed in Fig. 3. Note that the mobility is larger in the out-of-plane than in the in-plane direction and that no "saturated" mobility is attained with increasing strain, both of which facts being in contrast to the corresponding situation of electrons [12] ("in-plane" and "out-of-plane" refer to the direction parallel and perpendicular to the interface between the strained Si layer and the unstrained SiGe substrate). The ohmic in–plane mobility in strained Si grown on a $Si_{0.7}Ge_{0.3}$ substrate, i.e. in the configuration considered for the nonlinear regime in this paper, reaches a value of about 1600 $cm^2/(Vs)$ which is roughly a factor of three larger than in the unstrained case. As can be expected from the small light hole mass, which is in the strained case relevant for transport in contrast to the large heavy hole mass experienced by most holes in the unstrained case (see Fig. 1), the transient ballistic overshoot is much stronger in strained Si than in the unstrained case, as is shown in Fig. 4. This implies that classical device simulation must also include the energy balance equations in order to take the overshoot effect into account. For transport param-

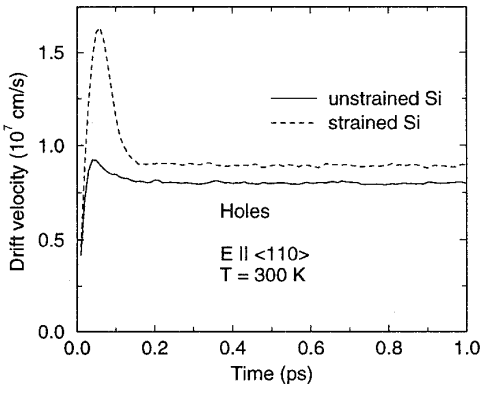

Figure 4: Transient in-plane velocity overshoot with a sudden application of a 100 kV/cm field parallel to the ⟨110⟩ direction at a lattice temperature of 300 K in unstrained Si and in strained Si grown on a $Si_{0.7}Ge_{0.3}$ substrate

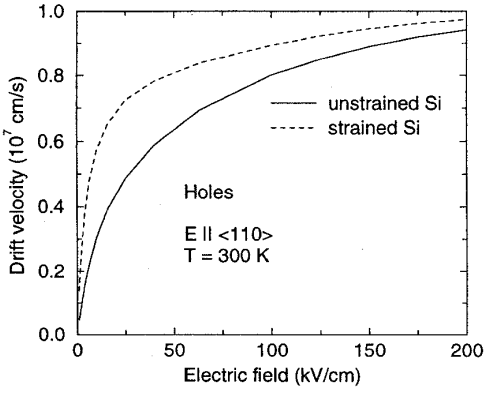

Figure 5: Velocity–field characteristics of holes with the field parallel to the ⟨110⟩ direction at a lattice temperature of 300 K in unstrained Si and in strained Si grown on a $Si_{0.7}Ge_{0.3}$ substrate

eters, it is therefore not sufficient to compute only the velocity–field characteristics of holes (which are displayed in Fig. 5 for unstrained and strained Si along the ⟨110⟩ direction relevant for actual devices). Note that the improvement present in the ohmic regime in Fig. 3 also extends to higher fields, but the saturation drift velocity is essentially the same. In Fig. 6, the drift velocity is plotted as a function of the equivalent hole temperature, which is defined by

$$\frac{3}{2}k_B T_{\text{hole}} \equiv w \tag{4}$$

with w denoting the mean energy which is needed for hydrodynamic device simulation. The initially surprising result is that the drift velocity in strained Si is always smaller than in unstrained Si. The reason is that the holes are much more easily heated in strained Si, as fol-

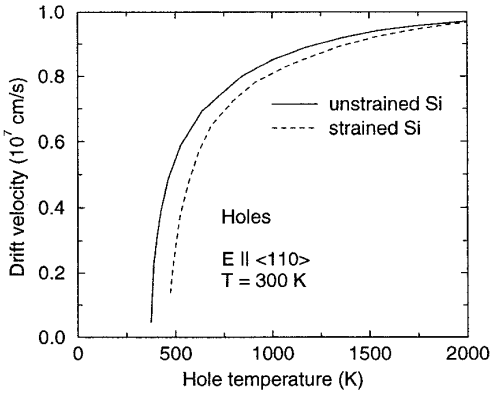

Figure 6: Drift velocities as a function of the hole temperature for the same situation as in Fig. 5

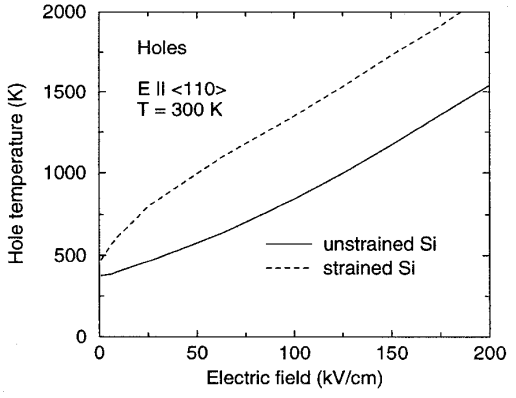

Figure 7: Hole temperatures as a function of the electric field for the same situation as in Figs. 5 and 6

lows from the relation between the hole temperature and the electric field, shown in Fig. 7. Hence, in unstrained Si, a much higher electric field corresponds to a given hole temperature in Fig. 6 and therefore the associated drift velocity is larger than in the strained case. This demonstrates that no conclusions for the transport properties of a material can be drawn from the velocity–temperature relation alone, since it is already clear from the energy dispersion in Fig. 1 that the transport properties in strained Si must be enhanced in comparison to the unstrained situation. Finally, the energy relaxation times in unstrained and strained Si are reported in Fig. 8. They can be seen to roughly change in the relevant high–field regime from 0.08 ps in unstrained Si to 0.12 ps in strained Si. However, the energy relaxation time deviates in the strained case at low hole temperatures much more from the high-temperature value than in the absence of strain.

4. Conclusions

In conclusion, we have presented realistic high–field transport parameters for use in hydrodynamic device sim-

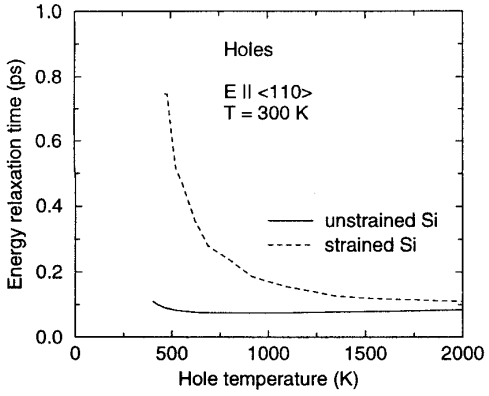

Figure 8: Energy relaxation times as a function of the hole temperature for the same situation as in Figs. 5, 6 and 7

ulation of submicron p–MOSFETs based on strained Si, i.e. the velocity–temperature relation as well as the energy relaxation time. The strongly enhanced transport properties compared to the unstrained case could be confirmed. The ohmic in-plane drift mobility of holes in (001)-strained Si grown on a $Si_{0.7}Ge_{0.3}$ substrate is about a factor three larger than in unstrained Si and the transient velocity overshoot for a sudden application of a 100 kV/cm field in ⟨110⟩ direction is improved by a factor of nearly two. The smaller drift velocity of strained Si found in the velocity–temperature relation could be traced back to the enhanced hole temperature for a given electric field.

Acknowledgments

We would like to thank M. M. Rieger for calculating the band structures and P. Vogl for useful discussions. This work was supported in part by the Bundesministerium für Bildung, Wissenschaft, Forschung und Technologie.

References

[1] D. K. Nayak, K. Goto, A. Yutani, J. Murota, and Y. Shiraki, IEEE Trans. Electron Devices **43**, 1709 (1996).

[2] S. Tiwari, M. V. Fischetti, P. M. Mooney, and J. J. Welser, in *Technical Digest of the International Electron Devices Meeting, Washington, DC, 1997*, p. 939.

[3] D. K. Nayak and S. K. Chun, Appl. Phys. Lett. **64**, 2514 (1994).

[4] M. V. Fischetti and S. E. Laux, J. Appl. Phys. **80**, 2234 (1996).

[5] J. E. Dijkstra and W. T. Wenckebach, J. Appl. Phys. **81**, 1259 (1997).

[6] F. M. Bufler, P. Graf, and B. Meinerzhagen, in Proceedings of the 5th International Workshop on Computational Electronics, Notre Dame, Indiana, May 1997, VLSI Design (to be published).

[7] M. M. Rieger and P. Vogl, Phys. Rev. B **48**, 14276 (1993).

[8] Y. Fu, K. J. Grahn, and M. Willander, IEEE Trans. Electron Devices **41**, 26 (1994).

[9] F. M. Bufler, *Full-Band Monte Carlo Simulation of Electrons and Holes in Strained Si and SiGe*. Munich: Herbert Utz Verlag, 1998 (http://utzverlag.com).

[10] M. A. Green, J. Appl. Phys. **67**, 2944 (1990).

[11] G. Ottaviani, L. Reggiani, C. Canali, F. Nava, and A. Alberigi-Quaranta, Phys. Rev. B **12**, 3318 (1975).

[12] F. M. Bufler, S. Keith, and B. Meinerzhagen, in *Proceedings of the Simulation of Semiconductor Processes and Devices Conference, Leuven (Belgium), 1998*, edited by K. De Meyer and S. Biesemans (Springer, Vienna, 1998), p. 239.